Dioxide, Oxygen, and Mixtures of Oxygen and Nitric Oxide," Twelfth Symposium (International) on Combustion, p. 469, The Combustion Institute (1969).
Solomon, P. R., and M. B. Colket, "The Evolution of Fuel Nitrogen in Coal Devolatilization," Unpublished Report (1978).
Sternling, C. V. and J. O. L. Wendt, "Kinetic Mechanisms Governing the Fate of Chemically Bound Sulfur and Nitrogen in Combustion," EPA-650/2-74-017 (1972).
Tarbell, J. M., and C. A. Petty, "Combustion Modifications for the Control of NO_x Emissions," *Chem. Engr. Sci.*, **32**(10), 1177 (1977).
Vogt, R. A., and N. M. Laurendeau, "Nitric Oxide Formation in Pulverized Coal Flames," Report No. PURDU-CL-76-8, Prepared for the National Science Foundation under Grant GK-42141 (1976).
Weekman, V. W., "Lumps, Models, and Kinetics in Practice," *AIChE Monograph Series*, **75** (1979).
Wen, C. Y., and St. Tone, "Coal Conversion Reaction Engineering," *ACS Symp. Ser.*, **72**, p. 56 (1978).
Wen, C. Y., R. C. Bailie, C. Y. Lin, and W. S. O'Brien, "Production of Low Btu Gas Involving Coal Pyrolysis and Gasification," *Adv. Chem. Ser.*, No. 131, p. 9 (1973).
Wendt, J. O. L., and D. W. Pershing, "Physical Mechanisms Governing the Oxidation of Volatile Fuel Nitrogen in Pulverized Coal Flames," *Comb. Sci. and Tech.*, **16**, 111 (1977).
Wendt, J. O. L., and O. E. Schulze, "On the Fate of Fuel Nitrogen During Coal Char Combustion," *AIChE J.*, **22**(1), 102 (1976).
Westenberg, A. A., Kinetics of NO and CO in Lean, Premixed Hydrocarbon-Air Flames," *Comb. Sci. and Tech.*, **4**, 59 (1971).
Williams, G. C., H. C. Hottel, and A. C. Morgan, "The Combustion of Methane in a Jet-Stirred Reactor," 12th Symposium (International) on Combustion, p. 913, The Combustion Institute (1976).
Zeldovich, J., "The Oxidation of Nitrogen in Combustions and Explosions," *Acta Physicochimica URSS*, **21**, 577 (1946).
Zimont, V. L., and Yu. M. Trushin, "Total Combustion Kinetics of Hydrocarbon Fuels," *Comb. Explosion and Shock Waves*, **5**(4), 391 (1969).

Manuscript received May 16, 1980; revision received April 30, and accepted May 15, 1981

Three-Dimensional, Randomized, Network Model for Two-Phase Flow through Porous Media

A structural model for a porous medium in the form of a randomized, three-dimensional network is developed that can be used to calculate permeability, capillary pressure as measured under static conditions and during steady-state flows, and relative permeabilities as measured during steady-state flows.

This randomized network model, expressed in terms of seven free parameters, can be employed to correlate for a given system the single-phase permeability, the drainage and imbibition capillary pressure curves, and the two drainage relative permeability curves. The subsequent portions of the hysteresis loops for capillary pressure and for the relative permeabilities then can be predicted.

The limited data available from the literature for unconsolidated packed beds have been successfully correlated: 100 to 200 mesh sand and uniform 181 μm glass spheres. Data for a bed of sintered 200 μm glass beads also has been successfully described.

CHENG-YUAN LIN
and
JOHN C. SLATTERY
Department of Chemical Engineering
Northwestern University
Evanston, IL 60201

SCOPE

The configuration of the pore space in a permeable rock, in a bed of sand, or in an irregular bed of spheres will normally be at least in part a random function of position in space. Although the usual equations of motion are believed applicable to each phase moving through an individual pore, they can not be solved, because an a priori description of the necessary boundary conditions is not possible.

The usual approach in avoiding this difficulty is to speak in terms of averaged variables. Formally, local volume averages of the equations of motion for each phase can be written that are valid for each point within a multiphase flow through a permeable structure. The advantages are that all local volume averaged variables are continuous functions of position in space and that detailed configurations for all of the various phase interfaces are no longer required.

The disadvantage is that in place of this lost information we have several integrals, descriptions for which must be given before we can proceed further. For a two-phase flow through a porous medium in the absence of interphase mass transfer, these integrals are the permeability to a single phase, the relative permeability for each phase, and the capillary pressure.

In describing these integrals, one can rely strictly on empiricism or correlations of experimental data. This is not entirely satisfactory, since there are many interacting physical phenomena.

Here we have adopted another approach in which these integrals are modelled through the introduction of an idealized structural model for the pore space bounded by the local averaging surface defined at each point within the porous medium. The model we have adopted is a three-dimensional, randomized network of sinusoidal pores. At each node in the network, we require mass conservation and continuity of pressure for each phase. A Beta probability density function is used to describe the distribution of the pore neck radii.

Such a model has not been used previously. Fatt (1956,a,b,c) employed a regular, two-dimensional network of cylindrical pores. His model was modified by Dodd and Kiel (1959) to allow

entrapment of the wetting phase in calculating the drainage capillary pressure. Chatzis and Dullien (1977) extended Fatt's (1956,a,b,c) model to three dimensions in computing the drainage capillary pressure, but they did not allow for entrapment of the wetting phase. Rose (1957) proposed that random interconnections in the network could be achieved by randomly blocking a portion of the pores, but he did not illustrate his idea with any calculations. The various statistical models (Scheidegger, 1954; de Josselin de Jong, 1958; Saffman, 1959; Haring and Greenkorn, 1970; Guin et al., 1971; Payatakes and Neira, 1977) and simplified network models (Dullien, 1975; Payatakes et al., 1977) do not formally recognize interconnections among the pores, in the sense that they do not require mass conservation and continuity of pressure for each phase at each interconnection. They can not account for bypassing and entrapment of the displaced phase, a nonzero irreducible saturation of the wetting phase at the conclusion of drainage, or a nonzero residual saturation of nonwetting phase at the conclusion of imbibition.

CONCLUSIONS AND SIGNIFICANCE

A structural model in the form of a randomized, three-dimensional network is developed that can be used to calculate permeability, capillary pressure as measured under static conditions and during steady-state flows, and relative permeabilities as measured during steady-state flows.

We suggest that this randomized network model, expressed in terms of seven free parameters, can be employed to correlate for a given system the single-phase permeability, the drainage and imbibition capillary pressure curves, and the two drainage relative permeability curves as measured during steady-state flows. The subsequent portions of the hysteresis loops for capillary pressure and for the relative permeabilities then can be predicted.

We have successfully correlated the limited data available from the literature for unconsolidated packed beds: 100 to 200 mesh sand (Leverett, 1939, 1941) and uniform 181 μm glass spheres (Topp and Miller, 1966). We also have successfully described data for sintered 200 μm glass beads (Topp and Miller, 1966).

We were not successful in using the randomized network model to correlate data for consolidated sandstones. The fact that they were consolidated may not be significant, since we did not have difficulty with the bed of sintered glass beads. It may be that our assumptions that the pore units were geometrically similar and that a correlation existed between pore length and pore neck radius were not justified for a naturally consolidated medium such as a sandstone. It may also be that the local probability density function for the pore size distribution varies significantly with position within a sample of naturally consolidated sandstone, in contrast with a basic assumption of our analysis.

This is the first time that a structural model has been successfully used to correlate for a given system the single-phase permeability, the drainage and imbibition capillary pressure curves, and the two relative permeability curves. This is the first time that a structural model has been successfully used to describe both the irreducible saturation of the wetting phase at the conclusion of drainage and the residual saturation of the nonwetting phase at the conclusion of imbibition. This is the first structural model capable of a quantitative prediction of the hysteresis loops for capillary pressure and the relative permeabilities.

This is also the first time that a structural model for a porous medium has been explicitly developed within the context of the local volume averaged equations of motion.

LOCAL VOLUME AVERAGING

Let us think for the moment about the flow of oil and water through a permeable rock. For most purposes, we are not particularly concerned with the detailed velocity distribution of each phase within a single pore. We may not care about the average velocity of the oil phase or the water phase within a single pore. We are more concerned with the variation of the average velocity of the oil and water phases as they move in the rock over distances that are large compared with the average diameter of a pore. Our primary concern is with averages defined for each phase at every position in the porous medium. The approach taken here is to speak in terms of local volume averages at each point in the structure (Slattery, 1967, 1968, 1969, 1970, 1981; Patel et al., 1972; Sha and Slattery, 1980; Anderson and Jackson, 1967; Whitaker, 1969, 1973; Bear, 1972; Bachmat, 1972; Gray, 1975; Gray and O'Neill, 1976; Gray and Lee, 1977; Hassanizadah and Gray, 1979).

Let us define V to be the volume of the region enclosed by the averaging surface S. We will denote by $R^{(i)}$ the region occupied by phase i within S; $V^{(i)}$ is the volume of phase i contained within S.

Assume that $B^{(i)}$ is some quantity associated with phase i. We will have occasion to speak of at least two averages (Slattery, 1967): the local volume average for phase i of $B^{(i)}$ (the mean value of $B^{(i)}$ in the region enclosed by S)

$$\overline{B}^{(i)} \equiv \frac{1}{V}\int_{R^{(i)}} B\, dV \tag{1}$$

and the intrinsic volume average for phase i of B (the mean value of B in $R^{(i)}$)

$$\langle B\rangle^{(i)} \equiv \frac{1}{V^{(i)}}\int_{R^{(i)}} B\, dV \tag{2}$$

Here dV denotes that a volume integration is to be performed.

Let us limit our attention here to creeping flows of incompressible, Newtonian fluids. The local volume average of Cauchy's first law for phase i is (Slattery, 1968, 1970; Sha and Slattery, 1980)

$$-\psi s^{(i)}\nabla\langle p\rangle^{(i)} + \operatorname{div}\underset{\approx}{\overline{S}}^{(i)} + \underset{\sim}{a}_m{}^{(i)} + \rho^{(i)}\underset{\sim}{b} = 0 \tag{3}$$

Here

$$\underset{\sim}{a}_m^{(i)} = \frac{1}{V}\int_{S_{\text{int}}^{(i)}} [(p^{(i)} - \langle p\rangle^{(i)})\underset{\approx}{I} - \underset{\approx}{S}^{(i)}]\cdot\xi^{(i)} dA \tag{4}$$

ψ is the local porosity, $s^{(i)}$ the local saturation of (volume fraction of the pore space occupied by) phase i, p pressure, $\underset{\approx}{S}$ the extra stress tensor or the viscous portion of the stress tensor, $\underset{\approx}{I}$ the identity tensor, ρ density, $\underset{\sim}{b}$ the body force (gravity) per unit mass, $S_{\text{int}}^{(i)}$ the portion of the closed surface bounding $R^{(i)}$ composed of phase interfaces, and $\xi^{(i)}$ the unit normal to $S_{\text{int}}^{(i)}$ pointing into phase i. Thinking of $\underset{\sim}{b}$ as gravity, we have treated it as a constant within the averaging region. In words, $-\underset{\sim}{a}_m^{(i)}$ is approximately the viscous force exerted on $S_{\text{int}}^{(i)}$ by phase i. An order of magnitude argument allows us to conclude that the second term can be neglected with respect to $\underset{\sim}{a}_m^{(i)}$ and Eq. 3 reduces to (Slattery, 1969, 1970; Sha and Slattery, 1980)

$$-\psi s^{(i)}\nabla\langle p\rangle^{(i)} + \underset{\sim}{a}_m{}^{(i)} + \psi s^{(i)}\rho^{(i)}\underset{\sim}{b} = 0 \tag{5}$$

In taking the local volume average of Cauchy's first law, we have introduced local volume averaged variables in the discussion and we have eliminated the necessity for an explicit description of the

pore geometry. However, as in any averaging process, information has been lost. We are now faced with the necessity of introducing an empirical relationship for $\underset{\sim}{a}_m^{(i)}$. A simple argument suggests that for isotropic porous media.

$$-\underset{\sim}{a}_m^{(i)} = \frac{\psi s^{(i)}\,\mu^{(i)}}{k k^{(i)*}}\,\underset{\sim}{v}^{(i)} \tag{6}$$

in which $\mu^{(i)}$ is the viscosity of phase i, k is the permeability of the porous structure to a single phase, $k^{(i)*}$ is the relative permeability of the structure to phase i. In view of Eq. 6, Eq. 5 can be written in the usual form of the extension of Darcy's law to multiphase flow in porous media:

$$-\nabla \langle p \rangle^{(i)} + \rho^{(i)}\,\underset{\sim}{b} = \frac{\mu^{(i)}}{k k^{(i)*}}\,\underset{\sim}{v}^{(i)} \tag{7}$$

Similarly, the local area average of the jump momentum balance at the interface between phase i and j requires (Slattery, 1968; Sha and Slattery 1980)

$$\langle p \rangle^{(i)} - \langle p \rangle^{(j)} = p_c^{(i,j)} \tag{8}$$

The capillary pressure function $p_c^{(i,j)}$ must be determined empirically.

RELATIVE PERMEABILITY

Relative permeabilities reported in the literature are derived from studies either of unsteady-state displacement (Johnson et al., 1959) or of steady-state flows (Osaba et al., 1951).

In an unsteady-state displacement, some of the fluid-fluid phase interfaces are moving. The relative permeabilities may be affected both by the properties of these interfaces as well as by the properties of the individual phases.

In a steady-state flow, the phase interfaces are stationary (Kimbler and Caudle, 1957). The relative permeabilities observed in such an experiment will not be explicit functions of interfacial behavior. But they may be implicit functions, since the saturation change between two successive steady-state flows is an unsteady-state displacement in which the interfacial properties may play important roles.

These considerations suggest that the measured relative permeabilities can be influenced by the design of the experiment.

Unsteady-state displacements of the nonwetting phase are often free or forced imbibitions, which result in it being trapped in the smaller pores (Handy and Datta, 1966; Slattery, 1974). The unsteady-state displacement of the nonwetting phase between successive steady-state flows in normally a restricted imbibition, which would result in it being trapped in the larger pores (Handy and Datta, 1966; Slattery, 1974). Handy and Datta (1966) found that for consolidated porous media the relative permeabilities measured using an unsteady-state displacement of the nonwetting phase differed from those determined using a steady-state flow. They suggested that the difference would depend upon the pore size distribution. The difference would be less for a narrow pore size distribution, since there would be less difference between the saturation histories.

If the wetting phase is being displaced, it will be trapped in the smaller of those pores initially containing it (Slattery, 1974). When the wetting phase is being displaced, the difference between a relative permeability measured using a steady-state flow and that determined using an unsteady-state displacement could be expected to be smaller, since there would be less difference between the saturation histories. This does not seem to have been investigated.

The effects of the viscosity ratio and of the magnitude of the pressure gradient upon the relative permeabilities appear to depend upon the design of the experiment. The fraction of the displaced phase trapped and stranded depends upon the ratio of the viscosity of the displacing phase to that of the displaced phase and upon the magnitude of the pressure gradient (Appendix A). This suggests that the relative permeabilities measured using an unsteady-state displacement will show a dependence upon both the viscosity ratio and the magnitude of the pressure gradient. But the unsteady-state displacements between successive steady-state flows are normally carried out so slowly that the effects of the viscous forces and of the magnitude of the pressure gradient upon the saturation history can be neglected with respect to those of the interfacial forces. The relative permeabilities determined using a steady-state flow would not be expected to show a dependence upon either the viscosity ratio or the magnitude of the pressure gradient. Using an unsteady-state displacement, Lefebvre du Prey (1970) found that the relative permeabilities he measured did depend upon the viscosity ratio. Using steady-state flows, Osaba et al. (1951), Sanberg et al. (1958), and Leverett (1939) concluded that the viscosity ratio has no effect on relative permeabilities; Odeh (1959) reported a similar conclusion for samples having large pores. Using unsteady-state displacements, Warren and Colhoun (1955), Peaz et al. (1955), and Lefebvre de Prey (1970) found that the relative permeabilities they measured did depend upon the magnitude of the pressure gradient. Using steady-state flows, Osaba et al. (1951) and Sandberg et al. (1958) concluded that, if boundary effects were minimized, the relative permeabilities were independent of the pressure gradient.

The relative permeabilities are found to be functions of the interfacial tension both in unsteady-state displacements (Warren and Colhoun, 1955; Peaz et al., 1955; Lefebvre du Prey, 1970) and in steady-state flows (Leverett, 1939; Batycky and McCaffery, 1978; Talash, 1976). Although the fraction of the displaced phase initially trapped is insensitive to the magnitude of the interfacial tension, the fraction of the displaced phase left stranded will decrease as the interfacial tension decreases (Slattery, 1974).

Starting with their porous media saturated with the wetting phase, Geffen et al. (1951), Sandberg et al. (1958), and Land (1971) concluded that, after the first drainage and imbibition, the relative permeability curves for the second drainage retraced those found during the first imbibition. But Evrenos and Comer (1969) and Colonna et al. (1972) found no such evidence of reversibility.

CAPILLARY PRESSURE

Capillary pressure may be derived from pressure measurements under static conditions (Bruce and Welge, 1947; Purcell, 1949), from pressure measurements during steady-state flows (Brown, 1951; Topp and Miller, 1966), and from measurements of saturation as a function of position under static conditions (Leverett, 1941).

Capillary pressure is an explicit function of interfacial tension. It is regarded as an explicit function of saturation instead of the mean curvature of the phase interfaces. Measured capillary pressures may be implicit functions of other variables, since the saturation change between two successive static conditions or steady-state flows is an unsteady-state displacement in which both the bulk and interfacial properties could play important roles.

This indicates that capillary pressure measurements can be influenced by the design of the experiment.

The unsteady-state displacement of the nonwetting phase between successive pressure measurements either under static conditions or during steady-state flows is normally a restricted imbibition; it will be trapped in the larger pores (Handy and Datta, 1966; Slattery, 1974). If the wetting phase is being displaced, it will be trapped in the smaller of those pores initially containing it (Slattery, 1974). This suggests that capillary pressures derived from pressure measurements under static conditions should be in close agreement with those derived from pressure measurements during steady-state flows, since they would have similar saturation histories. This is confirmed by Brown (1951). However, there is little reason to believe that they are identical.

Measurements of saturation as a function of position under static conditions normally follow a free imbibition of the wetting phase (Leverett, 1941). In a free imbibition, the nonwetting phase will be trapped in the smaller pores (Handy and Datta, 1966; Slattery,

1974). Since the saturation history would be different, this technique should be expected to give a different relationship for capillary pressure than either pressure measurements under static conditions (Bruce and Welge, 1947; Purcell, 1949) or pressure measurements during steady-state flows (Brown, 1951; Topp and Miller, 1966).

Unsteady-state displacements between successive pressure measurements either under static conditions or during steady-state flows are normally carried out so slowly that the effects of the viscous forces upon the saturation history can be neglected with respect to those of the interfacial forces (Leverett, 1941; Dumore and Schols, 1974).

Capillary pressure hysteresis has been recognized to be the result of contact angle hysteresis and irregularity of the pore structure (Melrose, 1965).

STRUCTURAL MODELS

That portion of a real porous medium included within an averaging surface S is a set of irregular pores of different sizes interconnected in a three-dimensional network. We will refer to idealizations of this network as structural models.

Fatt (1956a,b,c) introduced the first structural model in the form of a two-dimension network of cylindrical tubes. Capillary pressure and relative permeabilities during drainage were computed for several pore-size distributions and for several relations between pore radius and length. The model was modified by Dodd and Kiel (1959) to allow entrapment of the wetting phase in calculating capillary pressure as a function of saturation during drainage of the wetting phase. Chatzis and Dullien (1977) extended Fatt's (1956a,b,c) model to three dimensions in computing the drainage capillary pressure, but they did not allow for entrapment of the wetting phase. Rose (1957) proposed that random interconnections in the network could be achieved by randomly blocking a portion of the pores, but he did not illustrate his idea with any calculations.

As an alternative to the network model, Larson (1977) utilized percolation theory (Broadbent and Hammersley, 1957; Shante and Kirkpatrick, 1971; Kirkpatrick, 1973) to calculate the relative permeability curves in a Bethe tree network. Unfortunately, he assumes that all pores in the network have the same size.

Statistical models in which the pores are randomly oriented in space have been developed by Scheidegger (1954), by de Josselin de Jong (1958), by Saffman (1959), by Haring and Greenkorn (1970), by Guin et al. (1971), and by Payatakes and Neira (1977). These models do not rigorously recognize interconnections among the pores; they do not require equality of pore pressure and conservation of mass at interconnections. There is no allowance for the possibility that portions of the displaced phase may be bypassed and trapped, that there may be a nonzero irreducible saturation of wetting phase at the conclusion of drainage, or that there may be a nonzero residual saturation of nonwetting phase at the conclusion of imbibition.

The simplified network models employed by Dullien (1975) and by Payatakes et al. (1977) may be viewed as special cases of the statistical models. Rather than permitting the individual pores to be randomly oriented in space, these models identify the directions of the pores with the directions of bonds in a network, although equality of pore pressures and conservation of mass at nodes are not recognized.

Ehrlich and Crane (1969) demonstrated that hysteresis can be described qualitatively with a network of capillaries having interconnections. They constructed a simple four-pore series-parallel network to compute drainage and imbibition relative permeability curves from a given pore size distribution. Their results were qualitatively similar to experimental relative permeability curves.

In what follows, we show that a structural model in the form of a randomized, three-dimensional network can be used to correlate experimentally observed relative permeabilities and capillary pressures, including their hysteresis loops.

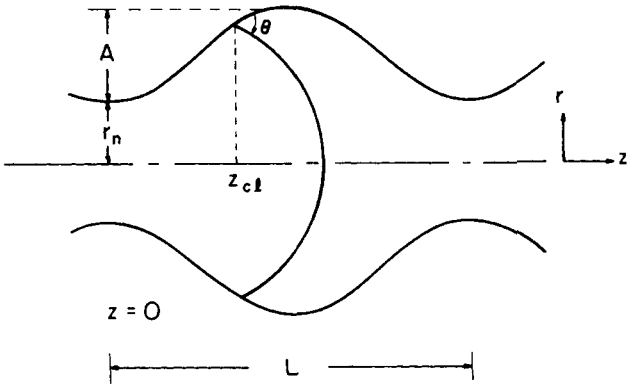

Figure 1. Configuration of sinusoidal pore.

RANDOMIZED NETWORK MODEL

In what follows, we develop a structural model in the form of a randomized, three-dimensional network that can be used to calculate permeability, capillary pressure as measured under static conditions and during steady-state flows (see CAPILLARY PRESSURE), and relative permeabilities as measured during steady-state (see RELATIVE PERMEABILITY).

We will require the following idealizations.

1) The basic representation for the pore structure enclosed by the averaging surface S is a randomized, three-dimensional, face-centered, cubic network. The bonds in the network represent the pores; the nodes or points of interconnection have zero volume and zero resistance to flow. The coordination number (number of pores intersecting at a node) of a face-centered, cubic network is 12. A randomly chosen portion of the pores are assigned zero volume; the average coordination number n of the randomized network is a free parameter.

2) A phase is continuous across a node, whenever two or more pores intersecting at the node are occupied by that phase. We require that the mass of each phase be conserved at each node. We also require that the pressure of each phase be single-valued at each node.

3) The pore radii are sinusoidal functions of axial position (Slattery, 1974; Oh and Slattery, 1979). Referring to Figure 1, we require that the pore units be geometrically similar

$$A^* \equiv \frac{A}{r_n} = \text{a constant}$$

$$L^* \equiv \frac{L}{r_n} = \text{a constant} \tag{9}$$

where r_n is the pore neck radius. This may be more reasonable for unconsolidated porous media than for naturally consolidated media such as sandstones. For convenience, a further restriction is placed upon A^* and L^* to insure that there will be no discontinuous movement (Oh and Slattery, 1979) of the interface during displacement. (See Eq. 21 and Appendix B.)

4) The total pore length L_t between two adjacent nodes is related to r_n by (Fatt, 1956a)

$$L_t = L_{t,\max}\left(\frac{r_n}{r_{n,\max}}\right)^a \tag{10}$$

Here $r_{n,\max}$ and $L_{t,\max}$ are the maximum pore neck radius and its corresponding pore length; a is a free parameter. As with Eq. 9, this may be more justified for unconsolidated porous media than for naturally consolidated media such as sandstones. We also assume that

$$V_t = V_u \frac{L_t}{L} \tag{11}$$

and

$$-\Delta p_t = -\Delta p_u \frac{L_t}{L} \tag{12}$$

where

V_t = volume of a pore between two nodes

V_u = volume of a unit pore (a pore of length L)

$-\Delta p_t$ = pressure drop across a pore between two nodes

$-\Delta p_u$ = pressure drop across a pore unit of length L

5) Pores are randomly distributed in the network by their neck radius r_n.

6) This random distribution of pores in the network is consistent with a probability density function $f[(r_n)/(r_{n,\max})]$ represented by the Beta distribution (Haring and Greenkorn, 1971)

$$f\left(\frac{r_n}{r_{n,\max}}\right) = \frac{\Gamma(\alpha+\beta+2)}{\Gamma(\alpha+1)\,\Gamma(\beta+1)}\left(\frac{r_n}{r_{n,\max}}\right)^{\alpha}\left(1-\frac{r_n}{r_{n,\max}}\right)^{\beta} \tag{13}$$

in which $\Gamma(x)$ is the Gamma function. The minimum r_n for the Beta distribution is zero. Since the probability density function normally is negligibly small for radii smaller than some finite value, a positive effective minimum r_n is obtained for the network as shown in Figure 4. The value of this effective minimum r_n depends on the values assigned α and β.

7) The porous medium is nonoriented or isotropic in the sense that there is no natural direction associated with the pore structure enclosed by an averaging surface.

8) Since the configuration of the averaging surface is arbitrary, we choose for convenience a cube.

9) For an isotropic porous medium, the capillary pressure, the permeability, and the two relative permeabilities do not depend upon the orientation of the averaging surface with respect to the gradients of the intrinsic volume averaged pressures. For convenience, we orient our cubic averaging surface such that one of the axes is parallel to the gradients of the intrinsic averaged pressures.

10) The capillary pressure, the permeability, and the two relative permeabilities do not depend upon the velocity distributions and pressure distributions outside the cubic averaging surface. For convenience, we say that, on the four sides of the cube parallel to the gradients of the intrinsic averaged pressures, there is no flow and that the pressures of both phases are constants on the inlet surface and on the outlet surface.

11) The region enclosed by the averaging surface is sufficiently large that Monte Carlo sampling errors are small.

12) The distribution of nonwetting phase and wetting phase during a displacement is determined by assuming that the capillary forces dominate the viscous forces. This is consistent with capillary pressure measurements made under static conditions and during steady-state flows (see CAPILLARY PRESSURE) and with relative permeabilities derived from steady-state flows (see RELATIVE PERMEABILITY).

13) The displacing phase will invade a pore, only if the pressure distribution is sufficient to allow it to completely replace the other phase in that pore. At equilibrium or during a steady-state flow, a pore will never be shared by two phases.

(14) A phase can be displaced from a pore, if and only if all of the following conditions are satisfied.

i) The applied pressure difference between the two phases satisfies the necessary condition for displacement.

ii) There is a continuous path of displacing phase from the inlet of the network to the inlet of the pore.

iii) There is a continuous path of the displaced phase from the outlet of the pore to the outlet of the network.

15) The displaced phase will be trapped, whenever the pores which it occupies are isolated by the displacing phase.

16) In a steady-state flow, all phase interfaces are stationary (Kimbler and Caudle, 1957). For this reason, the two phases can be treated separately in relative permeability computations.

17) Entrance and exit effects upon the pressure drop through an individual pore are ignored.

18) Because of assumptions 13 and 17, we do not attempt to satisfy LaPlace's equation at every phase interface during a steady-state flow. For the same reason, we make no attempt to see that Eq. 8 is satisfied during the steady-state flow computations, except at the entrance and exit to the system. We rely heavily upon assumption 12.

19) Inertial effects are neglected within individual pores.

20) The cubic averaging surface is sufficiently small that the effects of gravity can be neglected within the region it encloses.

21) Both the wetting phase and the nonwetting phase are incompressible, Newtonian fluids.

22) The interfacial tension, the advancing contact angle, the receding contact angle, and the viscosities of both phases are constants. The advancing and receding contact angles are normally unknown in porous media. If the equilibrium contact angle is less than 21.6°, Morrow's (1975) class III contact angle hysteresis suggests that both the advancing and receding contact angles are zero. For convenience, we will take both the advancing and receding contact angles to be zero, although we will see that this assumption has little effect upon the results.

23) In comparing our results with available experimental data, we assume that the probability density function $f[(r_n)/(r_{n,\max})]$, which describes the pore neck radius distribution within the region enclosed by the averaging surface, is independent of position.

CAPILLARY PRESSURE CALCULATION

The static pressure difference across a phase interface in a single pore, the radius of which is a sinusoidal function of axial position, is given by the LaPlace equation as (Oh and Slattery, 1979)

$$p^{(nw)} - p^{(w)} = \frac{2\gamma}{r_n} g(\theta, A^*, L^*, z^*) \tag{14}$$

where

$$g(\theta, A^*, L^*, z^*) \equiv \frac{\cos\theta + \left(\frac{A^*\pi}{L^*}\right)\sin\theta\,\sin\left(\frac{2\pi z}{L^*}\right)}{\left\{1+\frac{A^*}{2}\left[1-\cos\left(\frac{2\pi z^*}{L^*}\right)\right]\right\}\left\{1+\left(\frac{A^*\pi}{L^*}\right)^2\sin^2\left(\frac{2\pi z^*}{L^*}\right)\right\}^{1/2}} \tag{15}$$

$$z^* \equiv \frac{z}{r_n} \tag{16}$$

Here $p^{(nw)}$ is the pressure in the nonwetting phase, $p^{(w)}$ the pressure in the wetting phase, γ the interfacial tension, and θ the contact angle measured through the wetting phase. For a given set of θ, A^*, and L^*, $g(z^*)$ is a periodic function.

Prompted by Eq. 8, let us define the capillary pressure p_c for our two-phase system as

$$p_c \equiv \langle p\rangle^{(nw)} - \langle p\rangle^{(w)} \tag{17}$$

Capillary pressure is a function of both saturation and saturation history.

Let us begin with all of the pores space enclosed by the averaging surface filled with the wetting phase. This corresponds to saying that $p_c = 0$. At the inlet to the region enclosed by the averaging surface, increase p_c incrementally. There will be no displacement, until p_c exceeds some threshold value required to displace the wetting phase from the pore having the largest diameter of those pores which intersect the inlet. As p_c is increased above this threshold value, wetting phase is drained from the system and is replaced by the nonwetting phase. Since wetting phase is being drained from the system, we refer to the drainage capillary pressure and designate it as p_{cd}. For each incremental change in p_{cd} at the inlet, we compute the corresponding change in the saturation of the wetting phase by starting at the inlet, applying assumption 14, and recognizing that the wetting phase will be displaced from a pore only if

$$\frac{r_n}{r_{n,\max}} > \frac{2}{p_{cd}^*} \equiv \frac{2\gamma}{p_{cd} r_{n,\max}} \{\max [g(\theta_r, A^*, L^*, z^*)]\} \quad (18)$$

Here $\max[g(\theta_r, A^*, L^*, z^*)]$ is the maximum of g in $0 \le z^* < L^*$ for constant θ_r, A^*, and L^*; θ_r is the receding contact angle. As p_{cd} is increased, not all of the wetting phase will be displaced from the region enclosed by the averaging surface. There is an irreducible saturation of wetting phase corresponding to that portion of the wetting phase which has been bypassed and trapped according to assumption 15.

Starting from the irreducible saturation, let us now decrease p_c incrementally at the entrance for the averaging region. There again is a threshold value of p_c, above which the saturation of the wetting phase is unchanged. As p_c is decreased below this threshold value, the wetting phase imbibes, replacing the nonwetting phase. Since the wetting phase is imbibing into the system, we refer to the imbibition capillary pressure and designate it as p_{ci}. For each incremental change in p_{ci} at the inlet, we compute the corresponding change in the saturation of the wetting phase by starting at the inlet for imbibition, applying assumption 14, and recognizing that the nonwetting phase will be displaced from a pore only if

$$\frac{r_n}{r_{n,\max}} < \frac{2}{p_{ci}^*} \equiv \frac{2\gamma}{p_{ci} r_{n,\max}} \{\min [g(\theta_a, A^*, L^*, z^*)]\} \quad (19)$$

Here $\min [g(\theta_a, A^*, L^*, z^*)]$ is the minimum of g in $0 \le z^* < L^*$ for constant θ_a, A^*, and L^*; θ_a is the advancing constant angle. As p_{ci} is decreased to zero, not all of the nonwetting phase will be displaced from the region enclosed by the averaging surface. There is a residual saturation of nonwetting phase corresponding to that portion of the nonwetting phase which has been bypassed and trapped according to assumption 15. As we shall see shortly, the result will generally depend upon whether the inlet for imbibition corresponds to the inlet or exit for drainage.

Second drainage capillary pressure functions and second imbibition capillary pressure functions can be constructed in a similar fashion. Further hysteresis loops result from stoping short of either the irreducible saturation or residual saturation.

Given assumption 22, we see that

$$\max[g(\theta_r, A^*, L^*, z^*)] = 1 \quad (20)$$

When a wetting phase is displaced by a nonwetting phase, it is possible that a small portion of the wetting phase will be trapped as a ring along a portion of the pore wall (Oh and Slattery, 1979). This results in a discontinuous movement of the phase interface during the displacement (Oh and Slattery, 1979). Because of this entrapment, the imbibition after the first drainage will also have a discontinuous movement, which will affect the minimum of g. The position of the discontinuous movement and the volume of the trapped wetting phase depend upon θ_r, A^*, and L^*. When the receding contact angle is zero, the necessary and sufficient condition for continuous movement of the interface is (Appendix B)

$$A^*(1 + A^*) < \frac{L^{*2}}{2\pi^2} \quad (21)$$

If the pore geometry satisfies the above relation and if the advancing contact angle is zero, the minimum of g occurs at $z^* = 0.5L^*$ and

$$\min[g(\theta_a, A^*, L^*, z^*)] = \frac{1}{1 + A^*} \quad (22)$$

It will be shown later that the values of θ_a and θ_r have no effect on the shapes of the hysteresis loops which we predict.

SINGLE-PHASE PERMEABILITY CALCULATION

Neglecting inertia as well as the effects of the entrance and the exit, Neira and Payatakes (1979) have computed the volume rate of flow q through a sinusoidal pore of length L as [see also Fedkiw and Newman (1977) or Deiber and Schowalter (1979)]

$$q = \frac{\pi (r_n)^3 (-\Delta p_u)}{C \mu} \quad (23)$$

where

$$C \equiv \frac{\Delta P_1^*}{L^*} \quad (24)$$

and ΔP_1^* is taken from their Figure 1. For a pore of length L_t, Eqs. 10, 12 and 23 give

$$q^* \equiv q \frac{C \mu L_{t,\max}}{\pi (r_{n,\max})^4 L^* (-\Delta p_N)} = (-\Delta p_t^*) \left(\frac{r_n}{r_{n,\max}}\right)^{4-a} \quad (25)$$

in which

$$-\Delta p_t^* \equiv \frac{-\Delta p_t}{-\Delta p_N} \quad (26)$$

and $(-\Delta p_N)$ is the pressure drop over the network.

For a given network of pores and for a given pressure drop $(-\Delta p_N)$ over the network, the pressure and velocity distributions in the network are determined by requiring Eq. 25 to be satisfied in every pore, mass to be conserved at every node

$$\sum_{j=1}^{12} \left[(-\Delta p_t^*) \left(\frac{r_n}{r_{n,\max}}\right)^{4-a}\right]_j = 0 \quad (27)$$

and pressure to be single-valued at every node.

An integral momentum balance for the network shows us that

$$\int_{S_{\text{int}}} [(p - \langle p \rangle) \underset{\approx}{I} - \underset{\approx}{S}] \cdot \xi \, dA = (-\Delta p_N)(L_N)^2 \psi \frac{\bar{\underset{\sim}{v}}}{|\bar{\underset{\sim}{v}}|} \quad (28)$$

In writing this, we have neglected any viscous forces at the entrances and exits for the network. Because of the regularity of the network, $(L_N)^2 \psi$ represents the cross-sectional area available for flow at both the entrance and exit for the network, where

$$L_N \equiv \left(\frac{1}{\psi} \sum_{\text{ALL}} V_t\right)^{1/3} = \left[\frac{\pi}{\psi} (r_{n,\max})^2 L_{t,\max} \left(1 + A^* + \frac{3}{8} A^{*2}\right)\right]^{1/3} \left[\sum_{\text{ALL}} \left(\frac{r_n}{r_{n,\max}}\right)^{a+2}\right]^{1/3} \quad (29)$$

is the length of a side of the cubical averaging surface. In arriving at this last expression, we have used Eqs. 10, 11 and

$$V_u = \pi (r_n)^3 L^* \left(1 + A^* + \frac{3}{8} A^{*2}\right) \quad (30)$$

From Eqs. 4, 6, and 28, we conclude that the permeability of the network to a single phase is

$$k = \frac{\mu L_N |\bar{\underset{\sim}{v}}|}{-\Delta p_N} \quad (31)$$

The magnitude of the local volume averaged velocity for the network is

$$|\bar{\underset{\sim}{v}}| = \frac{1}{(L_N)^2} \sum_{\text{PLANE}} q \cos \varphi \quad (32)$$

with the understanding that φ is the angle between $\bar{\underset{\sim}{v}}$ and the axis of a pore in the network and the summation is taken over all pores in the network passing through a plane perpendicular to $\bar{\underset{\sim}{v}}$. With Eq. 32, we can rearrange Eq. 31 in the form

$$k^* \equiv k \frac{C \left\{\pi \left(1 + A^* + \frac{3}{8} A^{*2}\right)\right\}^{1/3} (L_{t,\max})^{4/3}}{\pi L^* \psi^{1/3} (r_{n,\max})^{10/3}} = q_N^* (V_N^*)^{-1/3} \quad (33)$$

where

$$q_N^* = \sum_{\text{PLANE}} q^* \cos\varphi \tag{34}$$

and

$$V_N^* \equiv \left[\pi\,(r_{n,\max})^2\, L_{t,\max}\left(1 + A^* + \frac{3}{8}A^{*2}\right)\right]^{-1} \times \sum_{\text{ALL}} V_t = \sum_{\text{ALL}} \left(\frac{r_n}{r_{n,\max}}\right)^{a+2} \tag{35}$$

RELATIVE PERMEABILITY CALCULATION

In a steady-state, two-phase flow, assumption 16 allows us to treat each phase separately. By assumption 12, the distribution of wetting phase and nonwetting phase in the network is determined in the corresponding capillary pressure calculation.

By analogy with the analysis we gave above for the single-phase permeability, we find

$$k^{(i)*} = \frac{q_N^{(i)*}}{q_N^*} \tag{36}$$

The dimensionless volume rate of flow of phase i through the network is

$$q_N^{(i)*} = \sum_{\text{PLANE}} q^{(i)*} \cos\varphi \tag{37}$$

with the summation now being taken over all pores filled with phase i passing through a plane perpendicular to $\bar{\varrho}$.

MONTE CARLO SOLUTION

A number of parameters have been introduced in the preceding sections: θ_a, θ_r, A^*, L^*, α, β, $r_{n,\max}$, $L_{t,\max}$, a, n, and the total number of pores in the network enclosed by the averaging surface. For the moment, let us assume that they all have been assigned values. In the next section, we will describe the manner in which we determined sub-optimal choices for these parameters.

For each set of computations, we began by randomizing a regular, face-centered, cubic network. A pseudo-random number generator of a uniform probability density function was used to generate random numbers between 0 and 1, one for each pore in the network. Those pores whose random number was less than $(1 - n/12)$ was assigned zero volumes. Any pores belonging to a cluster that was not accessible to fluid were assigned zero volume.

Pore radii were randomly assigned to those pores having nonzero volume. A pseudo-random number generator of a Beta probability density function was employed to generate a random number between 0 and 1 for each pore. This number was identified as $r_n/r_{n,\max}$.

The dimensionless total accessible pore volume V_N^* was calculated from Eq. 35.

In order to determine the pressure p^* at each node in single-phase flow through this network, we solved simultaneously all of the Eqs. 27 using Gauss-Seidel iteration. In doing so, we recognized that $p^* = 1$ at the entrance to the network, $p^* = 0$ at the exit from the network, and by assumption 10 there is no flow on the other four sides of the averaging surface bounding the network. This permitted us to compute the dimensionless volume rate of flow q_N^* through the network from Eqs. 25 and 34 and the dimensionless single-phase permeability k^* from Eq. 33.

Our next objective was to determine capillary pressure and the relative permeabilities during drainage. Starting from 100% wetting phase saturation and $p_{cd}^* = 0$, we increased p_{cd}^* in small increments. For each value of p_{cd}^*, the wetting phase saturation was determined by applying assumption 14 and inequality (Eq. 18). The volume of wetting phase trapped was computed using assumption 15. Recognizing assumptions 12 and 16, we employed Eq. 37 to calculate for each phase $q_N^{(i)*}$. We were able to determine the corresponding relative permeability $k^{(i)*}$ from Eq. 36. This was repeated for successive increments in p_{cd}^* until the irreducible saturation of wetting phase was reached.

Capillary pressure and the relative permeabilities during the imbibition were determined in a similar fashion. Starting from the irreducible saturation, p_{ci}^* was decreased in increments and the wetting phase was allowed to reimbibe into the network, displacing a portion of the nonwetting phase. For each value of p_{ci}^*, assumption 14 and inequality (Eq. 19) were applied to determine the wetting phase saturation.

The dimensionless capillary pressure and relative permeabilities during the second drainage were found in a similar manner to those for the first drainage, but starting from the residual nonwetting phase saturation. The dimensionless capillary pressure and relative permeabilities during the second imbibition were calculated in a manner analogous to those for the first imbibition.

Note that an infinite variety of additional hysteresis loops for capillary pressure and the two relative permeabilities can be found by terminating a drainage or imbibition at any intermediate saturation of the wetting phase.

Because we began each computation by constructing a randomized network with a randomly assigned pore size distribution, the computation had to be repeated a number of times so that meaningful averages could be reported. We normally repeated each computation ten times.

SUBOPTIMIZATION OF PARAMETERS

Our objective was to use the preceding Monte Carlo computation based upon our network structural model in order to correlate for a given system the single-phase permeability, the drainage and imbibition capillary pressure curves, and the drainage relative permeability curves. The parameters determined in this manner could then be used to predict the subsequent portions of the hysteresis loops for capillary pressure and for the relative permeabilities.

Some parameters were fixed on the basis of other considerations.

From Eqs. 18 and 19, we see that the advancing and receding contact angles θ_a and θ_r have no effect upon the predicted saturation distribution corresponding to a given capillary pressure that can not be balanced by adjusting the values chosen for A^* and L^*. As explained in assumption 22, we chose $\theta_a = \theta_r = 0$.

In our analysis, the choice of L^* has no effect that can not be balanced by adjusting the values of A^*, $r_{n,\max}$, and $L_{t,\max}$. Payatakes et al. (1973) estimated that $L^* = 5.2$ for a randomly packed bed of spheres and that $L^* = 5.5$ for a packed bed of sand. Fedkiew and Newman (1977) suggested that $L^* = 5.0$. For the sake of simplicity, we choose L^* to be so large as to preclude any discontinuous movement during drainage (Oh and Slattery, 1979). Inequality (Eq. 21) is satisfied for most porous media by setting $L^* = 6$, which was also suggested by Oh and Slattery (1979).

The number of pores in the network was taken to be sufficiently large that the Monte Carlo sampling error was small, yet sufficiently small that the computation time was reasonable. For the majority of this study, we used networks containing either 1,728 or 3,300 pores prior to randomization.

We see from Eqs. 18 and 19 that

$$p_{cd}^* = p_{cd}^*\,(s^{(i)}, \alpha, \beta, n, a) \tag{38}$$

$$p_{ci}^* = p_{ci}^*\,(s^{(i)}, \alpha, \beta, n, a) \tag{39}$$

In calculating the saturation, all dependence upon A^*, $r_{n,\max}$, and $L_{t,\max}$ is eliminated. From Eqs. 25, 27, 34, 36 and 37, we conclude that for both phases

$$k^{(i)*} = k^{(i)*}\,(s^{(i)}, \alpha, \beta, n, a) \tag{40}$$

The dimensional single-phase permeability does depend upon all seven remaining parameters:

$$k = k\,(\alpha, \beta, n, a, A^*, r_{n,\max}, L_{t,\max}) \tag{41}$$

It was not possible to determine optimal values of α, β, n, a, A^*, $r_{n,\max}$, and $L_{t,\max}$ using one of the standard optimization techniques. It was difficult to define an objective function, particularly since this was a lengthy Monte Carlo solution. (Given a network containing 1,728 pores and one set of parameters, it took 4–6 minutes of CDC 6600 computer time to compute one estimate of the first hysteresis loop for capillary pressure and the first hysteresis loops for the relative permeabilities.) We consequently adopted the following simpler approach.

For every set of α, β, n, and a, the parameters A^* and $r_{n,\max}$ were determined by fitting the experimental drainage capillary pressure curve and the experimental imbibition capillary pressure curve using Eqs. 18 and 19. The corresponding value of $L_{t,\max}$ was fixed by matching Eq. 33 to the experimental value of the single-phase permeability.

Where possible, the parameters n and a were subsequently fixed by requiring the predicted irreducible wetting phase saturation and residual nonwetting phase saturation to match the corresponding experimental results.

Starting with a smaller network (756 pores), we applied a simple pattern search to determine approximate values for α and β that would give the best fit of the drainage capillary pressure curve and the drainage relative permeability curves. We then switched to the normal size network to complete the search. We required the accuracy of our iteration to be of the same order as the Monte Carlo sampling error.

COMPARISON WITH AVAILABLE DATA

There are few experimental studies that have reported hysteresis loops both for capillary pressure and for the relative permeabilities.

100 to 200 Mesh Sand

In determining the capillary pressure curve for this system, Leverett (1939, 1941) measured saturation as a function of position under static conditions. He began with a free imbibition of the wetting phase, starting from zero wetting phase saturation. The displacement mechanism in this type of experiment is different from the restricted imbibition described in assumption 12 (Handy and Datta, 1966; Slattery, 1974). For that reason, his imbibition capillary pressure curve was given little weight in our suboptimization of parameters.

The parameters A^* and $r_{n,\max}$ were determined as previously described (see SUBOPTIMIZATION OF PARAMETERS) by fitting the experimental drainage capillary pressure curve and the experimental imbibition capillary pressure curve using Eqs. 18 and 19. In fitting the drainage capillary pressure curve, we determine

$$\frac{1}{r_{n,\max}}\{\max[g(\theta_r, A^*, L^*, z^*)]\}$$

and a relation between A^* and $r_{n,\max}$. In fitting the less reliable imbibition capillary pressure curve, we fix

$$\frac{1}{r_{n,\max}}\{\min[g(\theta_a, A^*, L^*, z^*)]\}$$

and the absolute values of A^* and $r_{n,\max}$. The absolute values of A^* and $r_{n,\max}$ affect only the value we assign $L_{t,\max}$ in matching the single-phase permeability; $L_{t,\max}$ plays no further role in our correlations.

The parameters α, β, n, and a were determined by comparing our theory with the drainage capillary pressure curve and the drainage relative permeability curves only.

The parameters found in this manner are

$\alpha = 3.0$ $\quad A^* = 0.434$

$\beta = 2.5$ $\quad r_{n,\max} = 1.87 \times 10^{-3}$cm

$n = 6.4$ $\quad L_{t,\max} = 2.98 \times 10^{-3}$cm

$a = -0.25$

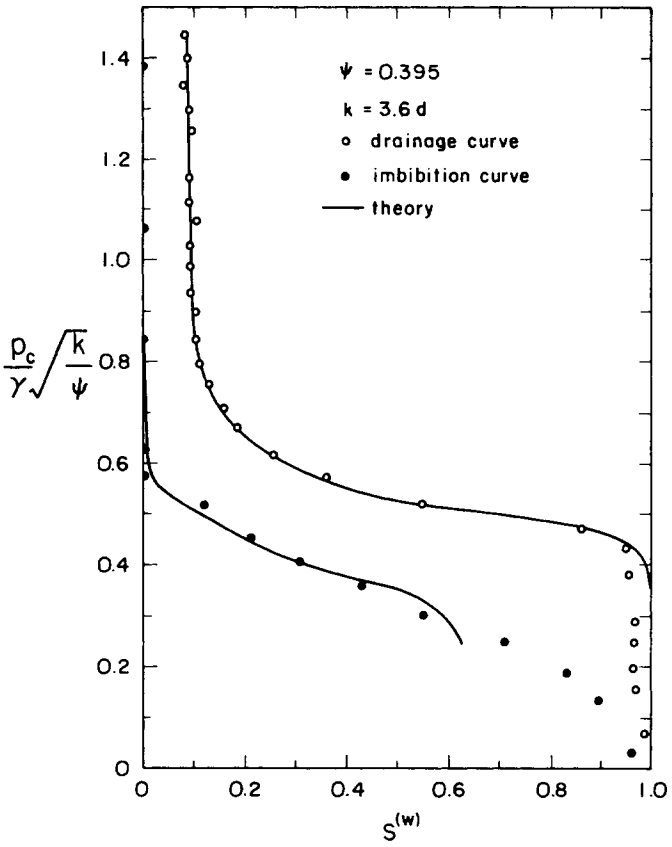

Figure 2. Comparison of capillary pressure from randomized network model with experimental data for 100 to 200 mesh sand (Leverett, 1941).

Figure 2 compares capillary pressure from the randomized network model with Leverett's (1941) experimental data. In a free imbibition, the nonwetting phase may be trapped preferentially in the smaller pores, especially when the capillary pressure is small (Handy and Datta, 1966; Slattery, 1974). When the capillary pressure is sufficiently small, this isolated nonwetting phase may be subsequently displaced. This may explain the observed residual nonwetting phase saturation being lower than represented by our theory.

Figure 3 compares the drainage relative permeabilities from the

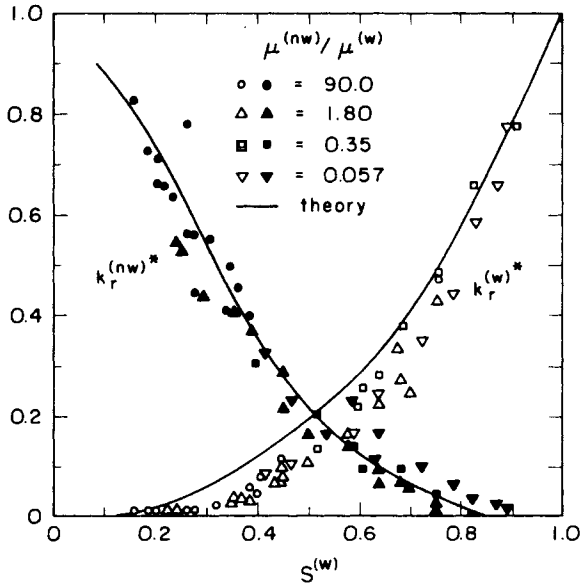

Figure 3. Comparison of drainage relative permeabilities from randomized network model with experimental data for 100 to 200 mesh sand (Leverett, 1939).

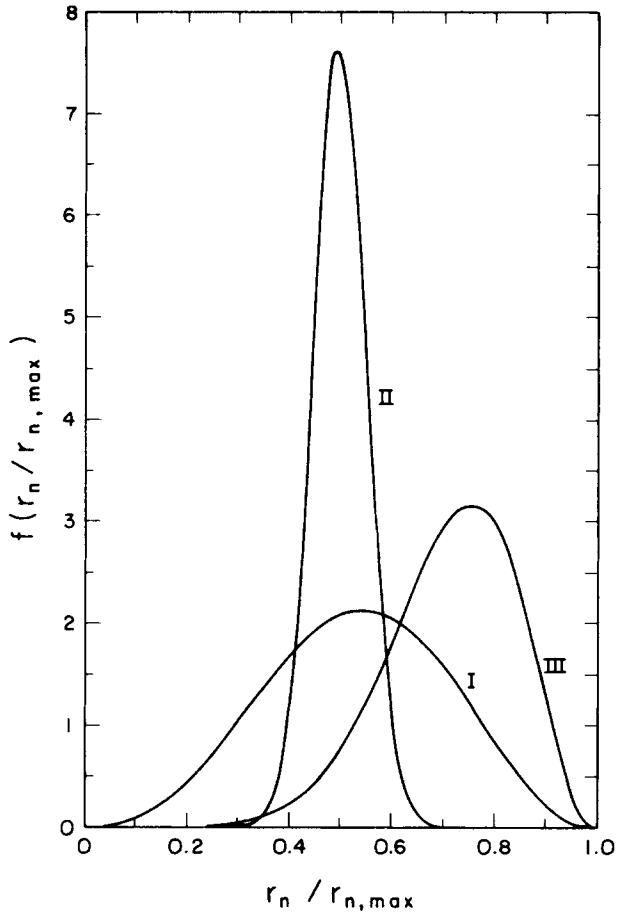

Figure 4. Probability density functions for the pore size distribution from the randomized network model. I: 100 to 200 mesh sand (Leverett, 1939, 1941). II: uniform glass spheres (Topp and Miller, 1966). III: sintered glass beads (Topp and Miller, 1966).

randomized network model with Leverett's (1939) experimental data. In agreement with the experimental studies, our theory predicts that the relative permeabilities measured in a steady-state experiment will not depend upon the viscosity ratio.

The probability density function for the pore size distribution is shown in Figure 4.

Figure 5 shows the capillary pressure hysteresis loops predicted for this system. In this computation, the inlet-outlet positions are switched for the phases for the imbibition after the first drainage is completed and for the second drainage after the imbibition is completed. The distribution of the imbibition is the same as that for the second drainage, since $p_{cd}^* = p_{ci}^*$ at the same saturation. The experimental hysteresis loops for this system are not available.

Land (1968, 1971) suggested that the relation between the initial nonwetting phase saturation and the residual nonwetting phase saturation can be correlated by

$$\frac{1}{s_r^{(nw)*}} - \frac{1}{s_i^{(nw)*}} = c \tag{42}$$

where

$$s_r^{(nw)*} \equiv \frac{s_r^{(nw)}}{1 - s_{ir}^{(w)}} \tag{43}$$

$$s_i^{(nw)*} \equiv \frac{s_i^{(nw)}}{1 - s_{ir}^{(w)}} \tag{44}$$

$s_r^{(nw)}$ is the residual nonwetting phase saturation, $s_i^{(nw)}$ the initial nonwetting phase saturation, $s_{ir}^{(w)}$ the irreducible wetting phase saturation, and c a constant characteristic of the porous media. Figure 6 compares the relationship between $s_r^{(nw)*}$ and $s_i^{(nw)*}$ that we predict for this system with Eq. 42 for $c = 1.436$. The deviations that we predict are in agreement with some typical experimental

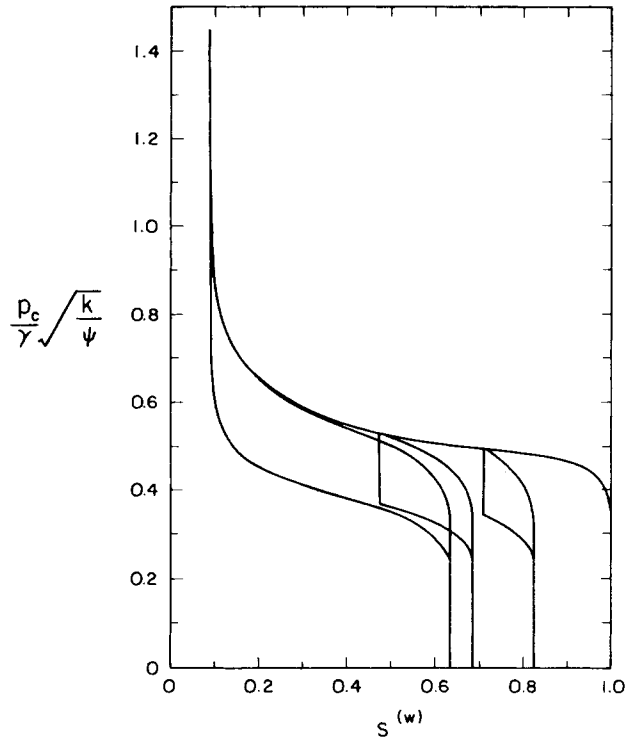

Figure 5. Capillary pressure hysteresis loops predicted by randomized network model for 100 to 200 mesh sand.

data (Land, 1971), which indicates that our assumptions about entrapment are reasonable.

The hysteresis loops for the relative permeabilities are given in Figure 7. After the imbibition is completed, the relative permeability curves are reversible; the second drainage curves retrace the imbibition curves. This agrees with some experimental results (Geffen et al., 1951; Sandberg et al., 1958; Land, 1971), but disagrees with others (Colonna et al., 1972; Evrenos and Comer, 1969).

Evrenos and Comer (1969) suggest that the hysteresis behavior observed depends upon the design of the experiment. In Figures 5 and 7, the inlet and outlet positions are reversed for the imbibition following completion of the first drainage and they are reversed again for the second drainage after completion of the imbibition. This procedure agrees with the experiment used to derive capillary pressure from pressure measurements under static conditions (Bruce and Welge, 1947; Purcell, 1949). But in experiments used to derive capillary pressure from pressure measurements during

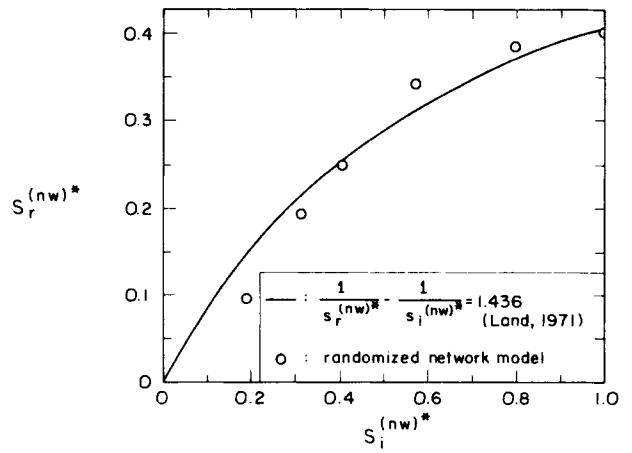

Figure 6. Relationship between initial and residual nonwetting phase saturations predicted by the randomized network model for 100 to 200 mesh sand.

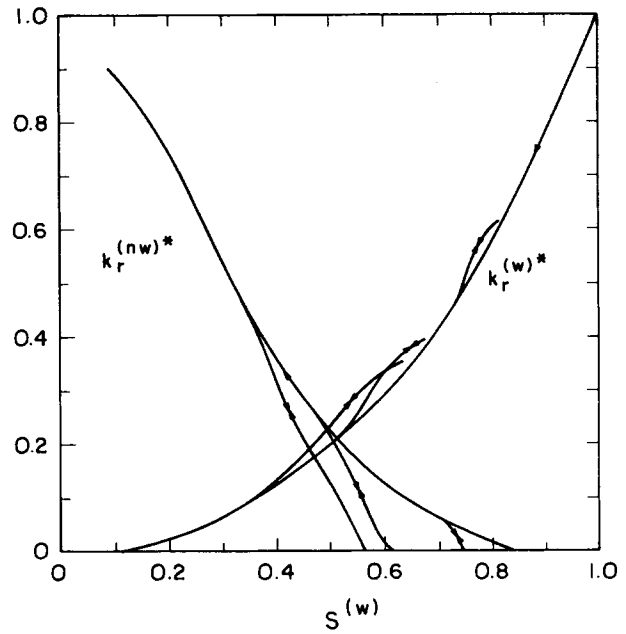

Figure 7. Hysteresis loops for relative permeabilities predicted by the randomized network model for 100 to 200 mesh sand.

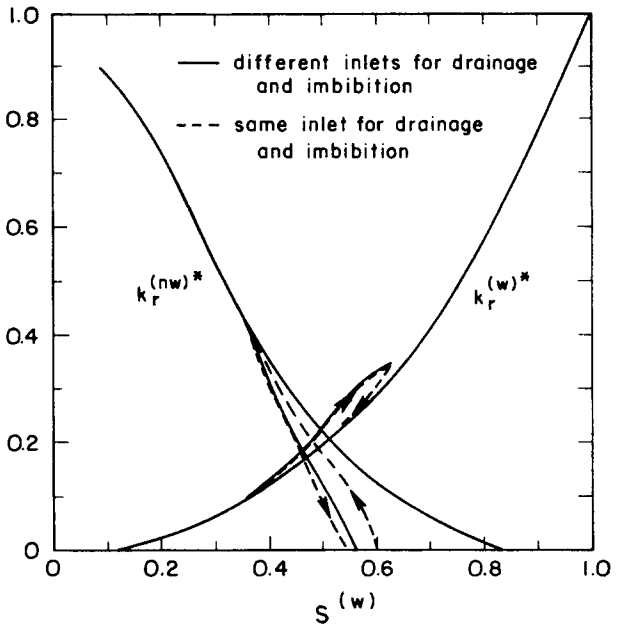

Figure 9. Effect of inlet positions on relative permeability hysteresis.

steady-state flows (Brown, 1951; Topp and Miller, 1966), the same inlet to core samples is used for both drainage and imbibition.

Figures 8 and 9 compare these two procedures. The most notable difference is that the second drainage relative permeability curves retrace the imbibition curves, when the inlet and outlet positions are reversed; they do not, when the same inlet is used for both drainage and imbibition. When the inlets are the same, the second drainage relative permeability for the wetting phase is lower than the imbibition relative permeability; the second drainage relative permeability for the nonwetting phase is higher than the imbibition relative permeability; the imbibition curve for the nonwetting phase ends with the saturation of the wetting phase at 0.55 and the second drainage curve begins at 0.60.

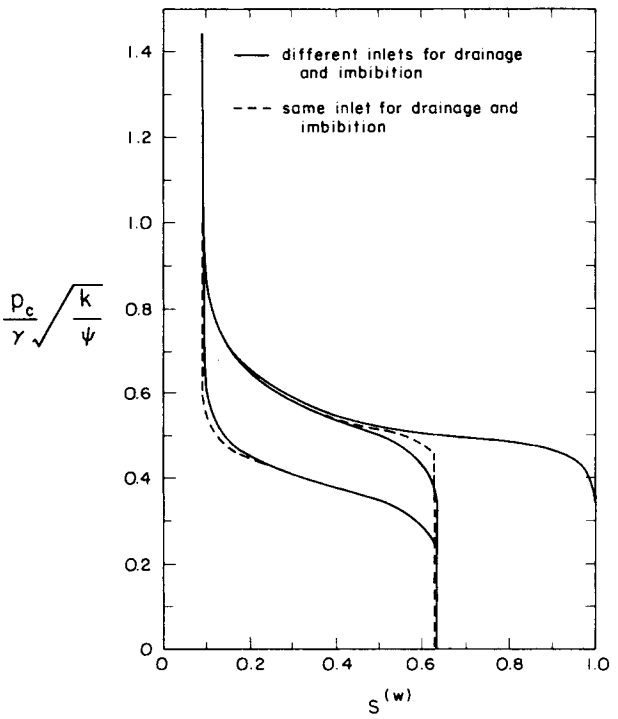

Figure 8. Effect of inlet positions on capillary pressure hysteresis.

In Figures 5 and 7 through 9, the imbibition process proceeds until the residual nonwetting phase saturation is reached, even though the residual nonwetting phase saturation is larger than the nonwetting phase saturation at which the nonwetting phase relative permeability goes to zero. This is consistent with the observations of Land (1971) and of Keelan and Pugh (1975). The explanation is that the wetting phase can continue to imbibe, when the relative permeability of the nonwetting phase is zero. In many experiments, the imbibition is terminated when the relative permeability of the nonwetting phase goes to zero. When we similarly terminated an imbibition and did not reverse the inlet and outlet, the second drainage relative permeability curves almost retraced those for imbibition. This together with normal experimental error may explain the apparent disagreement between experimentalists to which we referred above regarding the reversibility of the relative permeability curves.

Packed Uniform Spheres

Figure 10 and 11 show the hysteresis loops for capillary pressure and the relative permeabilities measured by Topp and Miller (1966) in a packed bed of uniform spheres, the diameter of which were 181 μm.

These figures also show the suboptimal fit of our theory to their hysteresis loop for capillary pressure and to their drainage relative permeability curves as well as our relative permeability curves predicted for imbibition. The parameters determined in the suboptimal fit of our theory to their data were

$$\alpha = 45 \qquad A^* = 0.736$$
$$\beta = 45 \qquad r_{n,\max} = 6.30 \times 10^{-3}\text{cm}$$
$$n = 10.2 \qquad L_{t,\max} = 8.18 \times 10^{-3}\text{cm}$$
$$a = -1.5$$

The probability density function for the pore size distribution shown in Figure 4 indicates uniform pores.

There is very little hysteresis in the relative permeabilities. This is in part attributable to the narrow pore size distribution. The small (large negative) value of a contributes by decreasing the effect of the breadth of the pore size distribution in Eq. 25.

Sintered Glass Beads

Figures 12 and 13 present the hysteresis loop for capillary pressure and the relative permeabilities determined by Topp and

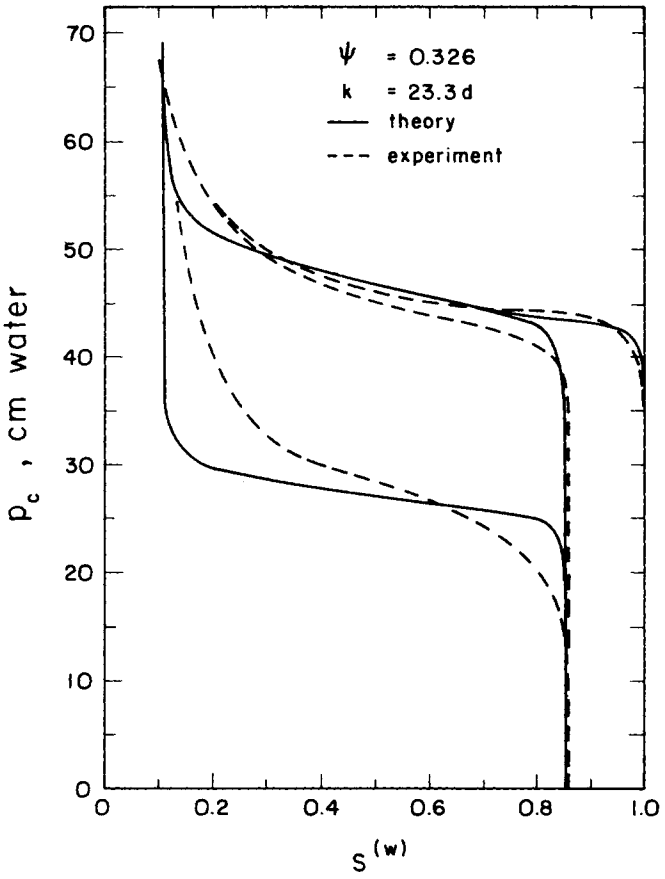

Figure 10. Comparison of capillary pressure from randomized network model with experimental data for uniform 181 μm glass spheres (Topp and Miller, 1966).

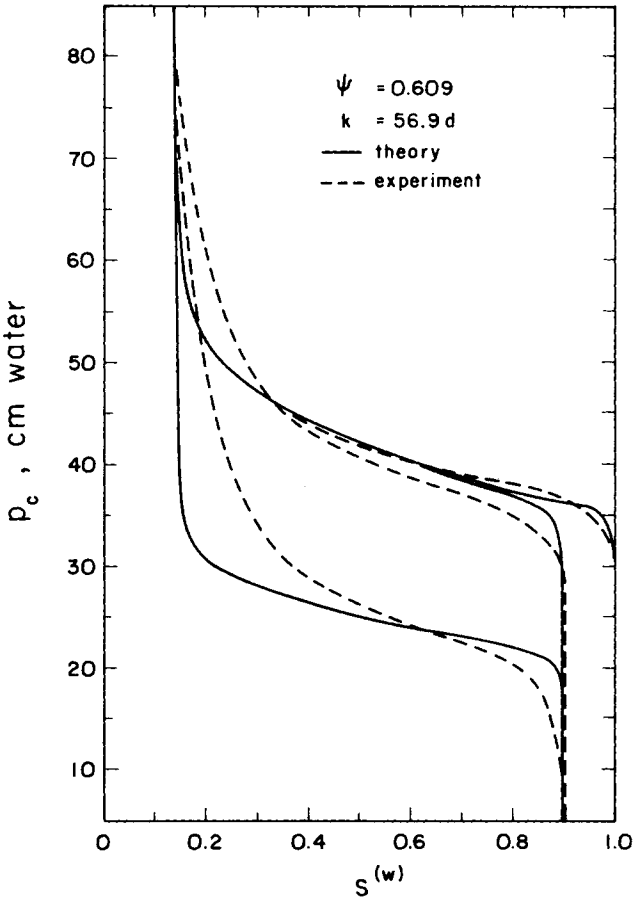

Figure 12. Comparison of capillary pressure from randomized network model with experimental data for sintered 200 μm glass beads (Topp and Miller, 1966)

Miller (1966) in a bed of sintered glass beads, the diameter of which were approximately 200 μm.

Also shown are the suboptimal fits of our theory to their hysteresis loop for capillary pressure and to their drainage relative permeability curves as well as our relative permeability curves predicted for imbibition. In the suboptimal fit of our theory to their data, we found

$$\alpha = 7.8 \qquad A^* = 0.676$$
$$\beta = 2.5 \qquad r_{n,\max} = 4.89 \times 10^{-3}\text{cm}$$
$$n = 10.5 \qquad L_{t,\max} = 9.48 \times 10^{-3}\text{cm}$$
$$a = -2.4$$

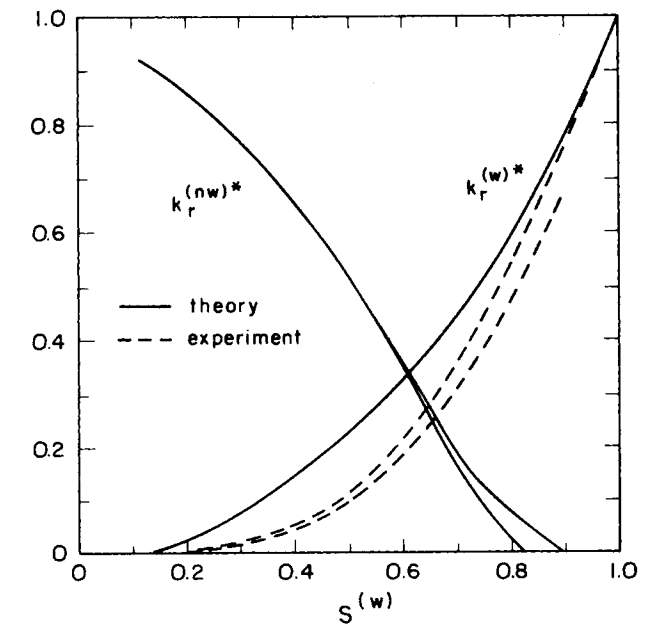

Figure 11. Comparison of relative permeabilities from randomized network model with experimental data for uniform 181 μm glass spheres (Topp and Miller, 1966).

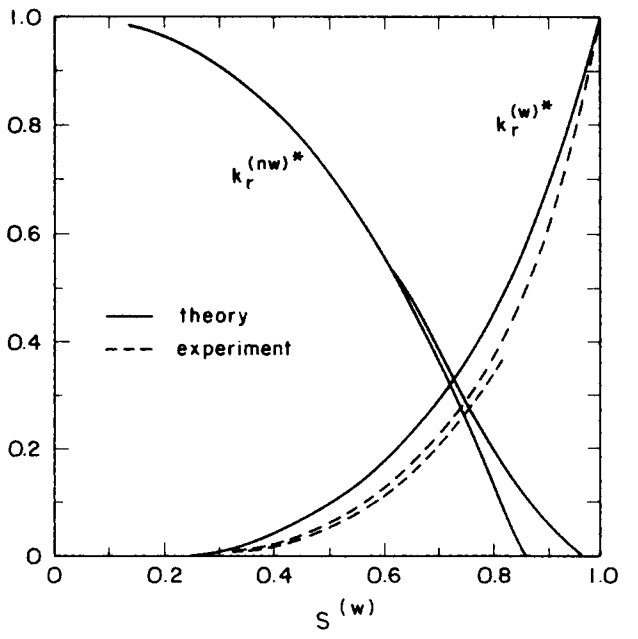

Figure 13. Comparison of relative permeabilities from randomized network model with experimental data for sintered 200 μm glass beads (Topp and Miller, 1966).

The corresponding probability density function for the pore size distribution is shown in Figure 4.

The deviations shown in Figures 12 and 13 are comparable to those in Figures 10 and 11, indicating no inherent difficulty with consolidated porous media.

ACKNOWLEDGMENT

The authors are grateful for financial support by the U.S. Department of Energy (Contact No. DE-AC19-79BC10068).

NOTATION

a = a free parameter in Eq. 10
$\underset{\sim}{a}_m^{(i)}$ = defined by Eq. 4
a_u = wall area of a pore unit of length L
A = amplitude of the sinusoidal function (Figure 1)
A^* = defined by Eq. 9
$\underset{\sim}{b}$ = acceleration of gravity
B = some quantity associated with phase i
$\overline{B}^{(i)}$ = local volume average for phase i of B, defined by Eq. 1
$\langle B\rangle^{(i)}$ = intrinsic volume average for phase i of B, defined by Eq. 2
C = defined by Eq. 24
c = a constant characteristic of the porous media in Eq. 42
f = probability density function
$\underset{\approx}{I}$ = identity tensor that transforms every spatial vector field into itself
k = permeability of the porous structure to a single phase
$k^{(i)*}$ = relative permeability of the porous structure to phase i
L = pore length of unit pore
L^* = defined by Eq. 9
L_N = length of a side of the cubical averaging surface
L_t = total pore length between two adjacent nodes
$L_{t,\max}$ = total pore length of the largest pore between two adjacent nodes
n = average coordination number of the randomized network
p = pressure
p^* = dimensionless pressure defined as $p/(-\Delta p_N)$
p_{cd} = drainage capillary pressure
p_{cd}^* = dimensionless drainage capillary pressure defined by Eq. (18)
p_{ci} = imbibition capillary pressure
p_{ci}^* = dimensionless imbibition capillary pressure defined by Eq. 19
$p_c^{(i,j)}$ = capillary pressure function
$p^{(nw)}$ = pressure in the nonwetting phase
$p^{(w)}$ = pressure in the wetting phase
$\langle p\rangle^{(i)}$ = intrinsic volume average for phase i of pressure
q = volume rate of flow through a sinusoidal pore of length L
q^* = dimensionless volume rate of flow through a sinusoidal pore of length L, defined by Eq. 25
q_N^* = total dimensionless volume rate of flow through the network
$q_N^{(i)*}$ = total dimensionless volume rate of flow of phase i through the network
r_n = pore neck radius
$r_{n,\max}$ = maximum pore neck radius
r_s = configuration of the fluid-fluid interface in a sinusoidal pore when the receding contact angle is zero and $z_{c\ell} = L/2$
r_s^* = defined as r_s/r_n
$R^{(i)}$ = region occupied by phase i within the averaging surface
$s^{(i)}$ = local saturation of phase i
$s_i^{(nw)}$ = initial nonwetting phase saturation
$s_i^{(nw)*}$ = dimensionless initial nonwetting phase saturation, defined by Eq. 44
$s_r^{(nw)}$ = residual nonwetting phase saturation
$s_r^{(nw)*}$ = dimensionless residual nonwetting phase saturation, defined by Eq. 43
$s_{ir}^{(w)}$ = irreducible wetting phase saturation
S = averaging surface
$\underset{\approx}{S}$ = extra stress tensor
$S_{\text{int}}^{(i)}$ = portion of the closed surface bounding $R^{(i)}$ composed of phase interfaces
$\overline{\underset{\approx}{S}}^{(i)}$ = local volume average for phase i of extra stress tensor
t = time
$\underset{\sim}{v}$ = velocity vector
$\overline{\underset{\sim}{v}}^{(i)}$ = local volume average for phase i of velocity
V = volume enclosed by the averaging surface
$V^{(i)}$ = volume of phase i contained by the averaging surface
V_N^* = total dimensionless pore volume in the network, defined by Eq. 35
V_t = volume of a pore between two nodes
V_u = volume of a pore unit
z = cylindrical coordinate
z^* = dimensionless cylindrical coordinate defined by Eq. 16
$z_{c\ell}$ = position of common line or three-phase line of contact for advancing phase interface in Figure 1

Greek Letters

α = a free parameter in Eq. 13
β = a free parameter in Eq. 13
γ = interfacial tension
θ = contact angle measured through the wetting phase
θ_a = advancing contact angle
θ_r = receding contact angle
Γ = gamma function
φ = angle between $\underset{\sim}{v}$ and the axis of a pore in the network
ψ = local porosity
$\rho^{(i)}$ = density of phase i
$\mu^{(i)}$ = viscosity of phase i
$\xi^{(i)}$ = unit normal to $S_{\text{int}}^{(i)}$ pointing into phase i

Others

div = divergence operation
∇ = gradient operator
dA = indicating that an area integration is to be performed
dV = indicating that a volume integration is to be performed
$-\Delta p_N$ = pressure drop over the network
$-\Delta p_t$ = pressure drop across a pore between two nodes
$-\Delta p_t^*$ = defined by Eq. 26
$-\Delta p_u$ = pressure drop across a pore unit of length L
ΔP_1^* = dimensionless pressure difference taken from Figure 1 of Neira and Payatakes (1979).

LITERATURE CITED

Anderson, T. B., and R. Jackson, "A Fluid Mechanical Description of Fluidized Beds," *Ind. Eng. Chem. Fundam.*, **6**, 527 (1967).

Bachmat, Y., "Spatial Macroscopization of Processes in Heterogeneous Systems," *Isr. J. Technol*, **10**, 391 (1972).

Batycky, J. P., and F. G. McCaffery, "Low Interfacial Tension Displacement Studies," paper no. 78-29-26, 29th Annual Technical Meeting of the Petroleum Society of CIM, Calgary (June 13–16, 1978).

Bear, J., *Dynamics of Fluids in Porous Media*, American Elsevier, New York, (1972).
Broadbent, S. R., and J. M. Hammersley, "Percolation Processes I. Crystals and Mazes," *Proc. Cambridge Philos. Soc.*, **53**, 629 (1957).
Brown, H. W., "Capillary Pressure Investigations," *Trans. AIME*, **192**, 67 (1951).
Bruce, W. A., and H. J. Welge, "Restored-State Method for Determination of Oil in Place and Connate Water," *Oil & Gas J.*, **46**, 223 (1947).
Chatzis, I., and F. A. L. Dullien, "Modelling Pore Structure by 2-D and 3-D Networks with Application to Sandstones," *J. Can. Pet. Technol.*, **16**(1), 97 (1977).
Colonna, J., F. Brissaud, and J. L. Millet, "Evolution of Capillary and Relative Permeability Hysteresis," *Soc. Pet. Eng. J.*, **12**, 28 (1972).
Deiber, J. A., and W. R. Schowalter, "Flow Through Tubes with Sinusoidal Axial Variations in Diameter," *AIChE J.*, **25**, 638 (1979).
de Josselin de Jong, G, "Longitudinal and Transverse Diffusion in Granular Deposits," *Trans. Am. Geophys. Union.*, **39**, 67 (1958).
Dodd, C. G., and O. G. Kiel, "Evaluation of Monte Carlo Methods in Studying Fluid-Fluid Displacement and Wettability in Porous Rock," *J. Phys. Chem.*, **63**, 1646 (1959).
Dullien, F. A. L., "New Network Permeability Model of Porous Media," *AIChE J.*, **21**, 299 (1975).
Dumoré, J. M., and R. S. Schols, "Drainage Capillary-Pressure Functions and the Influence of Connate Water," *Soc. Pet. Eng. J.*, **14**, 437 (1974).
Ehrlich, R., and F. E. Crane, "A Model for Two-Phase Flow in Consolidated Materials," *Soc. Pet. Eng. J.*, **9**, 221 (1969).
Evrenos, A. I., and A. G. Comer, "Numerical Simulation of Hysteretic Flow in Porous Media," SPE 2693, 44th Annual Fall Meeting of the Society of Petroleum Engineers of AIME, Denver, CO (Sept. 28–Oct. 1, 1969).
Fatt, I., "The Network Model of Porous Media I. Capillary Pressure Characteristics," *Trans. AIME*, **207**, 144 (1956a).
Fatt, I., "The Network Model of Porous Media II. Dynamic Properties of a Single Size Tube Network," *Trans. AIME*, **207**, 160 (1956b).
Fatt, I., "The Network Model of Porous Media III. Dynamic Properties of Networks with Tube Radius Distributions," *Trans. AIME*, **207**, 164 (1956c).
Fedkiew, P., and J. Newman, "Mass Transfer at High Peclet Numbers for Creeping Flow in a Packed-Bed Reactor," *AIChE J.*, **23**, 255 (1977).
Geffen, T. M., W. W. Owens, D. R. Parrish, and R. A. Morse, "Experimental Investigation of Factors Affecting Laboratory Relative Permeability Measurements," *Trans. AIME*, **192**, 99 (1951).
Gray, W. G., "A Derivation of the Equations for Multi-Phase Transport," *Chem. Eng. Sci.*, **30**, 229 (1975).
Gray, W. G., and K. O'Neill, "On the General Equations for Flow in Porous Media and Their Reduction to Darcy's Law," *Water Resour. Res.*, **12**, 148 (1976).
Gray, W. G. and P. C. Y. Lee, "On the Theorems for Local Volume Averaging of Multiphase Systems," *Int. J. Multiphase Flow*, **3**, 333 (1977).
Guin, J. A., D. P. Kessler, and R. A. Greenkorn, "Average Pore Velocities in Porous Media," *Phys. Fluids*, **14**, 181 (1971).
Guin, J. A., D. P. Kessler, and R. A. Greenkorn, "The Permeability Tensor for Anisotropic Non-uniform Porous Media," *Chem. Eng. Sci.*, **26**, 1475 (1971).
Handy, L. L., and P. Datta, "Fluid Distributions during Immiscible Displacements in Porous Media," *Soc. Pet. Eng. J.*, **6**, 261 (1966).
Haring, R. E., and R. A. Greenkorn, "A Statistical Model of a Porous Medium with Nonuniform Pores," *AIChE J.*, **16**, 477 (1972).
Hassanizadeh, M., and W. G. Gray, "General Conservation Equations for Multi-Phase Systems: 1. Averaging Procedure," *Adv. Water Resour.*, **2**, 131 (1979).
Johnson, E. F., D. P. Bossler, and V. O. Naumann, "Calculation of Relative Permeability from Displacement Experiments," *Trans. AIME*, **216**, 370 (1959).
Keelan, D. K., and V. J. Pugh, "Trapped-Gas Saturation in Carbonate Formations," *Soc. Pet. Eng. J.*, **15**, 149 (1975).
Kimbler, O. K., and B. H. Caudle, "New Technique for Study of Fluid Flow and Phase Distribution in Porous Media," *Oil & Gas J.*, **55** (50), 85 (1957).
Kirkpatrick, S., "Percolation and Conduction," *Rev. Mod. Phys.*, **45**, 574 (1973).
Land, C. S., "Calculation of Imbibition Relative Permeability for Two and Three-Phase Flow from Rock Properties," *Soc. Pet. Eng. J.*, **8**, 149 (1968).
Land, C. S., "Comparison of Calculated with Experimental Imbibition Relative Permeability," *Soc. Pet. Eng. J.*, **11**, 419 (1971).
Larson, R. G., "Percolation in Porous Media with Application to Enhanced Oil Recovery," M.S. Thesis, University of Minnesota (1977).
Lefebvre du Prey, E. J., "Factor Affecting Liquid-Liquid Relative Permeabilities of a Consolidated Porous Medium," SPE 3039, 45th Annual Fall Meeting of the Society of Petroleum Engineers of AIME, Houston, TX (Oct. 4–7, 1970).
Leverett, M. C., "Flow of Oil-Water Mixtures through Unconsolidated Sands," *Trans. AIME*, **132**, 149 (1939).
Leverett, M. C., "Capillary Behavior in Porous Solids," *Trans. AIME*, **142**, 152 (1941).
Melrose, J. C., "Wettability as Related to Capillary Action in Porous Media," *Soc. Pet. Engl J.*, **5**, 259 (1965).
Morrow, N. R., "The Effects of Surface Roughness on Contact Angle with Special Reference to Petroleum Recovery," *J. Can. Pet. Technol*, **14** (4), 42 (1975).
Neira, M. A., and A. C. Payatakes, "Collocation Solution of Creeping Newtonian Flow through Sinusoidal Tubes," **25**, 725 (1979).
Odeh, A. S., "Effect of Viscosity Ratio on Relative Permeability," *Trans. AIME*, **216**, 346 (1959).
Oh, S. G., and J. C. Slattery, "Interfacial Tension Required for Significant Displacement of Residual Oil," *Soc. Pet. Eng. J.*, **19**, 83 (1979).
Osaba, J. S., J. G. Richardson, J. K. Kerver, J. A. Hafford and P. M. Blair, "Laboratory Measurements of Relative Permeability," *Trans. AIME*, **192**, 47 (1951).
Payatakes, A. C., C. Tien, and R. M. Turian, "A New Model for Granular Porous Media," *AIChE J.*, **19**, 58 (1973).
Payatakes, A. C., and M. A. Neira, "Model of the Constricted Unit Cell Type for Isotropic Granular Porous Media," *AIChE J.*, **23**, 922 (1977).
Payatakes, A. C., R. W. Flumerfelt, and K. M. Ng, "Model of Isotropic Partition and Coalescence During Immiscible Displacement," paper presented at the AIChE 70th Annual Meeting, New York (Nov. 13–17, 1977).
Patel, J. G., M. G. Hegde, and J. C. Slattery, "Further Discussion of Two-Phase Flow in Porous Media," *AIChE J.*, **18**, 1062 (1972).
Peaz, J., P. Reed, and J. C. Calhoun, "Relationship Between Oil Recovery, Interfacial Tension, Pressure Gradient and Water-Wet Porous Media," *Prod. Mon.*, **19**, 34 (May, 1955).
Purcell, W. R., "Capillary Pressures—Their Measurements Using Mercury and the Calculation of Permeability Therefrom," *Trans. AIME*, **186**, 39 (1949).
Rose, W., "Studies of Waterflood Performance III. Use of Network Models," *ILL. State Geol. Surv. Circ.*, No. 237 (1957).
Saffman, P. G., "A Theory of Dispersion in a Porous Medium," *J. Fluid Mech*, **6**, 321 (1959).
Sandberg, C. R., L. S. Gournay, and R. F. Sippel, "The Effect of Fluid-Flow Rate and Viscosity on Laboratory Determinations of Oil-Water Relative Permeabilities," *Trans. AIME*, **213**, 36 (1958).
Scheidegger, A. E., "Statistical Hydrodynamics in Porous Media," *J. Appl. Phys.*, **25**, 994 (1954).
Sha, W. T., and J. C. Slattery, "Local Volume-Time Averaged Equations of Motion for Dispersed, Turbulent, Multiphase Flows," NUREG/CR—1491, ANL-80-51, Argonne National Laboratory, Argonne, ILL 60439 (1980).
Shante, V. K. S., and S. Kirkpatrick, "An Introduction to Percolation Theory," *Adv. Phys.*, **20**, 325 (1971).
Slattery, J. C., "Flow of Viscoelastic Fluids through Porous Media," *AIChE J.*, **13**, 1066 (1967).
Slattery, J. C., "Multiphase Viscoelastic Flow through Porous Media," *AIChE J.*, **14**, 50 (1968).
Slattery, J. C., "Single-Phase Flow Through Porous Media," *AIChE J.*, **15**, 866 (1969).
Slattery, J. C., "Two-Phase Flow Through Porous Media," *AIChE J.*, **16**, 345 (1970).
Slattery, J. C., "Interfacial Effects in the Entrapment and Displacement of Residual Oil," *AIChE J.*, **20**, 1145 (1974).
Slattery, J. C., "Interfacial Effects in the Displacement of Residual Oil by Foam," *AIChE J.*, **25**, 283 (1979).
Slattery, J. C., *Mometum, Energy, and Mass Transfer in Continua*, McGraw-Hill, New York (1972), second ed., R. E. Krieger, Malabar, FL (1981).
Talash, A. W., "Experimental and Calculated Relative Permeability Data for Systems Containing Tension Additives," SPE 5810, paper presented at SPE-AIME Symposium on Improved Oil Recovery, Tulsa, OK (March 22–24, 1976).
Topp, G. C., and E. E. Miller, "Hysteretic Moisture Characteristics and Hydraulic Conductivities for Glass-Bead Media," *Soil Sci. Soc. Am. Proc.*, **30**, 156 (1966).
Warren, J. E., and J. C. Calhoun, "A Study of Waterflood Efficiency in Oil-Wet Systems," *Trans. AIME*, **204**, 22 (1955).
Whitaker, S., "Advances in Theory of Fluid Motion in Porous Media," *Ind. Eng. Chem.*, **61** (12), 14 (1969).
Whitaker, S., "The Transport Equations for Multi-Phase Systems," *Chem. Eng. Sci.*, **28**, 139 (1973).

APPENDIX A: ENTRAPMENT OF DISPLACED PHASE

Slattery (1974 and 1979) used an integral momentum balance as the basis for predicting the qualitative effects of several variables upon the entrapment of a displaced phase. Here we wish to extend that argument to include the effects of the viscosity ratio and the magnitude of the pressure gradient.

Let us begin by slightly modifying Eq. 16 of Slattery (1974) to read

$$v^*_{(o)} \equiv \frac{v_{(o)}\mu_{(o)}}{|\nabla \langle p \rangle^{(o)}|^2} = \frac{R^{*2}A - R^* N_\gamma B}{F + R^* N_{\kappa+\epsilon} E} \tag{A-1}$$

in which we have defined

$$N_\gamma \equiv \frac{\gamma}{|\nabla \langle p \rangle^{(o)}|^2}$$

$$A \equiv \frac{\Delta p}{|\nabla \langle p \rangle^{(o)}|} - \mathcal{F}_z^{(p)*}$$

$$F \equiv 2L^*_{(o)} \mathcal{F}^{(v)*}_{(o)} + 2(1 - L^*_{(o)}) \frac{\mu_{(w)}}{\mu_{(o)}} \mathcal{F}^{(v)*}_{(w)}$$

$$L^*_{(o)} \equiv \frac{L_{(o)}}{\ell}$$

$$\mathcal{F}^{(v)*}_{(o)} \equiv \frac{\mathcal{F}^{(v)}_{(o)}}{2\pi L_{(o)} \mu_{(o)} v_{(o)}}$$

$$\mathcal{F}^{(v)*}_{(w)} \equiv \frac{\mathcal{F}^{(v)}_{(w)}}{2\pi (\ell - L_{(o)}) \mu_{(w)} v_{(o)}} \tag{A-2}$$

Retaining as much of the original notation as possible, we will understand here that $|\nabla \langle p \rangle^{(o)}|$ is the magnitude of the gradient of the local volume average of pressure for the oil phase, ℓ is the length of an individual pore, $L_{(o)}$ is the length of the segment of displaced phase (oil) remaining in a pore at any given time, $\mu_{(o)}$ is the viscosity of the displaced phase (oil), $\mu_{(w)}$ is the viscosity of the displacing phase (water), $\mathcal{F}^{(v)}_{(o)}$ is the z component of the viscous force exerted by the displayed phase (oil) on that portion of the pore wall in contact with the displaced phase, and $\mathcal{F}^{(v)}_{(w)}$ is the z component of the viscous force exerted by the displacing phase (water) on that portion of the pore wall in contact with the displacing phase. All other quantities are defined by Slattery (1974), which must be consulted for the background required to understand the arguments that follows.

For our present purposes, we will ignore the effects of the surface viscosities and set $N_{\kappa+\epsilon} = 0$. Consider

$$\frac{\partial^2 v^*_{(o)}}{\partial(\mu_{(w)}/\mu_{(o)})\partial R^*} = -\frac{2}{F}(1 - L^*_{(o)}) \mathcal{F}^{(v)*}_{(w)} \frac{\partial v^*_{(o)}}{\partial R^*} \tag{A-3}$$

The sign of this term must be the opposite of $\partial v^*_{(o)}/\partial R^*$, which leads us to conclude in the context of Slattery (1974):

The fraction of the displaced phase trapped will descrease as the ratio of the viscosity of the displacing phase to the viscosity of the displaced phase is increased.

In a similar manner, consider

$$\frac{\partial^2 (v^*_{(o)} N_\gamma^{-1})}{\partial N_\gamma^{-1} \partial R^*} = \frac{\partial v^*_{(o)}}{\partial R^*} + N_\gamma \frac{B}{F} \tag{A-4}$$

Slattery (1974) would argue that more of the displaced phase will be trapped, when this derivative has the same sign as $\partial v^*_{(o)}/\partial R^*$. For displacement of oil by water in oil-wet rock, both $\partial v^*_{(o)}/\partial R^*$ and B are positive; for restricted displacements of oil by brine in water-wet rock, both are negative (Slattery, 1974). We conclude:

The fraction of oil trapped in either oil-wet rock or in a restricted displacement through a water-wet rock will be enhanced by increasing the magnitude of the pressure gradient.

No conclusion can be drawn regarding free or forced displacement of oil by water in a water-wet rock, unless we are willing to assume that the pores are right, circular cylinders.

APPENDIX B: DERIVATION OF EQ. 21

When a wetting phase is displaced in a sinusoidal pore by a nonwetting phase, the possibility of a discontinuous movement depends on the pore geometry and the receding contact angle (Oh and Slattery, 1979). As A^* decreases, the position of the advancing interface ($z_{c\ell}$ in Figure 1) at which the discontinuous movement occurs increases, the region of discontinuous movement decreases, and the volume of the trapped wetting phase also decreases. If A^* is so small that the interface can advance to the position of the maximum diameter ($z_{c\ell} = L/2$) without touching the pore wall, the discontinuous movement will never occur. The necessary and sufficient condition for continuous movement is that, when $z_{c\ell} = L/2$, the fluid-fluid interface intersects the pore wall in only a single common line or three-phase line of contact.

When the receding contact angle is zero and $z_{c\ell} = L/2$, the configuration on the interface in cylindrical coordinates is given by

$$r^*_s \equiv \frac{r_s}{r_n} = [(1 + A^*)^2 - (z'^*)^2]^{1/2} \tag{B-1}$$

in which

$$z'^* \equiv z^* - 0.5L^* \tag{B-2}$$

The shape of the pore wall in cylindrical coordinates is

$$r^*_w \equiv \frac{r_w}{r_n} = 1 + \frac{A^*}{2}\left[1 + \cos\left(\frac{2\pi z'^*}{L^*}\right)\right] \tag{B-3}$$

The necessary and sufficient condition for continuous movement is that, at $z'^* = 0$, $(r_w - r_s)$ is a minimum. This implies

$$\text{at } z'^* = 0\text{: } \frac{d(r^*_w - r^*_s)}{dz'^*} = 0 \tag{B-4}$$

and

$$\text{at } z'^* = 0\text{: } \frac{d^2(r^*_w - r^*_s)}{dz'^{*2}} > 0 \tag{B-5}$$

Equation B-4 is satisfied identically; Eq. B-5 yields Eq. 21.

Manuscript received August 28, 1980; revision received April 17, and accepted May 6, 1981